Fourier Transform Infrared Spectra of a Late Intermediate of the Bacteriorhodopsin Photocycle Suggest Transient Protonation of Asp-212[†]

Andrei K. Dioumaev,[‡] Leonid S. Brown,[‡] Richard Needleman,[§] and Janos K. Lanyi*,[‡]

Department of Physiology and Biophysics, University of California, Irvine, California 92697, and Department of Biochemistry, Wayne State University, Detroit, Michigan 48201

Received April 15, 1999; Revised Manuscript Received May 17, 1999

ABSTRACT: We measured time-resolved difference spectra, in the visible and the infrared, for the Glu-194 and Glu-204 mutants of bacteriorhodopsin and detected an anomalous O state, labeled O′, in addition to the authentic O intermediate, before recovery of the initial state in the photocycle. The O′ intermediate exhibits prominent bands at 1712 cm^{-1} (positive) and 1387 cm^{-1} (negative). These bands arise with the same time constant as the deprotonation of Asp-85. Both bands are shifted to lower frequency upon labeling of the protein with [4-^{13}C]aspartic acid. The former band, but not the latter, is shifted in D_2O. These shifts identify the two bands as the carboxyl stretch of a protonated aspartic acid and the symmetric carbonyl stretch of an unprotonated aspartate, respectively, and suggest that in O′ an initially anionic aspartate enters into protonation equilibrium with Asp-85. Elimination of the few other candidates, on various grounds, identifies Asp-212 as the unknown residue. It is possible, therefore, that in the last step of the photocycle of the mutants studied the proton released from Asp-85 is conducted to the extracellular surface via Asp-212. An earlier report of a weak band at 1712 cm^{-1} late in the wild-type photocycle [Zscherp and Heberle (1997) *J. Phys. Chem. B 101,* 10542−10547] suggests that Asp-212 might play this role in the wild-type protein also.

Most of the proton-transfer reactions in the photocycle of bacteriorhodopsin, the light-driven proton pump (*1*−*3*), have been described in considerable detail. Protonation of Asp-85 upon deprotonation of the Schiff base of the all-trans to 13-cis photoisomerized retinal is followed by release of a proton from a location within a network of protein residues and bound water (*1*−*6*) to the extracellular membrane surface. The Schiff base is then reprotonated by Asp-96, and Asp-96 is in turn reprotonated from the cytoplasmic membrane surface. Upon the thermal reisomerization of the retinal to all-trans that ensues, Asp-85 transfers its proton to the extracellular proton release site (*7*, *8*) and thereby completes the full translocation of a proton across the membrane. The complex structure of the extracellular region (*6*) has made it difficult to describe the details of the proton movements, but there is strong evidence (*4*, *9*) that coupling exists between the protonation states of Asp-85 and the proton release site. This coupling accounts both for the decrease of the pK_a of the proton release site, leading to its dissociation when Asp-85 becomes protonated in the photocycle, and for the rise of the pK_a of Asp-85 when the proton is released to the extracellular surface. The side chains of Arg-82 (*10*−*12*), Glu-194 (*13*, *14*), and Glu-204 (*13*, *14*) are all necessary participants in the coupling, either directly or through their interactions with hydrogen-bonded water molecules (*5*, *6*, *15*).

Reestablishment of the initial state of bacteriorhodopsin in the last step of the photocycle is limited by the deprotonation of Asp-85, driven presumably by recovery of its initial low pK_a (*7*, *8*). Indeed, recent results have suggested that the rate constant of the decay of the last intermediate, the O state, is determined by the occupancy of the site that receives this proton, i.e., the proton release site (*16*). The proton transfer from Asp-85 at this time to either the proton release site (at pH > 5, the approximate pK_a for proton release) or directly to the surface (at pH < 5) is likely to utilize, at least partly, the interactions in the extracellular hydrogen-bonded network that regulate the pK_a of the proton release earlier in the photocycle. This is suggested by the finding that both proton release and decay of the O state exhibit uniquely high (6−10×) kinetic deuterium isotope effects (*8*, *11*, *17*, *18*). Further, in the E194Q and E204Q mutants, where the normal proton release is blocked, the decay of O is considerably (about 10×) slower than in the wild type (*14*, *19*). Finally, in the E194D mutant, where the pK_a for the proton release is higher than in the wild type (*14*), the pH dependency of the decay of the O state is described also with a higher pK_a (*16*). In molecular terms, however, the pathway of the proton after it leaves Asp-85 is not yet understood.

We report here evidence from Fourier transform infrared (FTIR) spectra that in the E194Q and E204Q mutants Asp-212, a residue that remains anionic during the most of the photocycle (*20*, *21*), becomes transiently protonated during deprotonation of Asp-85. Thus, in these mutants at least, Asp-

[†] This work was funded partly by grants from the National Institutes of Health (GM 29498 to J.K.L.), the Department of Energy (DEFG03-86ER13525 to J.K.L.), and the U.S. Army Research Office (DAAL03-92-G-0406 to R.N.).

* Correspondence should be addressed to this author: E-mail jlanyi@orion.oac.uci.edu.

[‡] University of California.

[§] Wayne State University.

10.1021/bi990873+ CCC: $18.00
Published on Web 07/15/1999

212 may be a participant in the conduction of the proton away from Asp-85. Since an IR band at the frequency we now assign to the protonated C=O stretch of Asp-212 had been detected, although with much lower amplitude, in the O state of the wild-type protein as well (*22*), Asp-212 may be the proton acceptor to Asp-85 during its deprotonation in the unperturbed photocycle as well.

MATERIALS AND METHODS

Purple membranes were prepared from *Halobacterium salinarum* by a standard method (*23*). The E194Q, E204Q, E194Q/E204Q, D96N/E194Q, E194D/E204Q, E9Q/E194Q, E194R, F208N, T205V, and T89A mutants were constructed as described before (*24*) and isolated after expression in *H. salinarum* as purple membrane patches. The cells were grown for [4-^{13}C] labeling of aspartates according to ref *25*.

Samples for the FTIR measurements were prepared by drying approximately 16 nmol of the protein on a CaF_2 window under mild vacuum. After drying, the films were soaked for 30−40 min in 50 mM MES or succinate buffer at pH/pD = 5.3 in the presence of 1 M NaCl (pD = pH + 0.41, where pH is the pH-meter reading). When higher pH was desired, PIPES buffer was used instead. This procedure is as described previously (*14*) but with the important modification that the films were not dried after soaking. Instead, the samples were sealed in a fully wet state, squeezing out the excess of buffer by pressing the second CaF_2 window. A 15 μm Teflon spacer (Spectra-Tech Inc., Shelton, CT) was used to fix the sample thickness. Approximately 45% ± 15% of the volume of the samples was liquid. All measurements were done at 8 °C, in a temperature-controlled sample holder (Harrick, Ossining, NY) connected to a water bath (RTE−111, Neslab, Portsmouth, NH). The FTIR time-resolved measurements were performed under OPUS software on a step-scan IR spectrometer (IFS-66s, Bruker, Germany) at 2 cm^{-1} resolution. Interferograms were collected in the "rapid-scan single side" mode (1888 points for 0−2000 cm^{-1} range) at 10.1 cm/s scanner velocity. The IR detector was equipped with a 2000 cm^{-1} cutoff filter (Optical Coating Laboratory, Inc., Santa Rosa, CA). The first 10 scans after laser excitation were recorded without coadding, providing 10 time points at 76 ms intervals, the next 10 time points by coadding 2 scans, the next 10 by coadding 4 scans, and so on, thereby creating a quasilogarithmic time base. Excitation was provided by the second harmonics of the Nd−YAG laser (Surelite II or Minilite II, Continuum, Santa Clara, CA) at 532 nm, with ~7 ns pulse width, and ~2 mJ/cm^2 pulse energy.

Kinetic analysis was done with a program (*26*) that simultaneously globally fitted arrays of 900 × 50 points (wavenumbers × times). The number of statistically valid exponentials was determined with *F*-test statistics. Spectra for "virtual states", which should have been measured if the cycle could be frozen between the apparent decays, were calculated from the amplitude spectra of the global fits. These spectra are not the true intermediate spectra (due to the presence of back-reactions) but rather spectra of mixtures of intermediates that are transformed into one another with the time constants of the apparent transitions (see also ref *27*).

The extent of [4-^{13}C] labeling of aspartates was less than 100%, as evident from Figures 7−10. The contributions of the labeled and unlabeled portions could be separated on the basis that all FTIR signals in the 1730−1800 cm^{-1} region originate from Asp-85, Asp-96, and Asp-115 during the photocycle. The spectra corresponding to fully [4-^{13}C]Asp-labeled sample were therefore calculated by interactive subtraction of the unlabeled spectra from the labeled ones until the frequency region between 1730 and 1800 cm^{-1} was virtually flat.

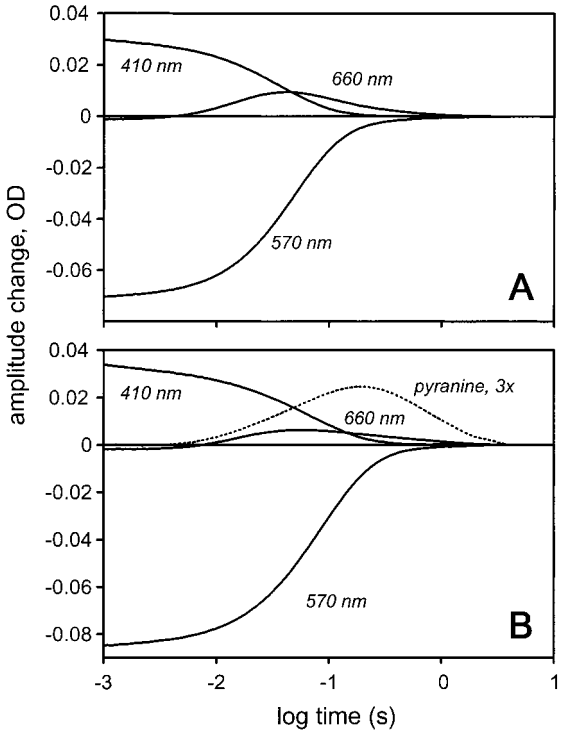

FIGURE 1: Time course of absorption changes after flash photoexcitation of the E9Q/E194Q mutant. (A) Measurement in 1 M NaCl, 25 mM succinate, *plus* 25 mM Bis-tris propane at pH 5.3. These conditions correspond to those used in the FTIR measurements but are carried out with membranes encased in acrylamide gel. (B) Measurement in 1 M NaCl, pH 6.5, membranes in suspension. Proton kinetics were calculated from traces with and without 50 μM pyranine.

Kinetic measurements in the visible were done as described earlier, either on the same films prepared for FTIR, immediately before or after those measurements, or on membranes in suspension or encased in polyacrylamide gel. For more details, and for measurements of time-resolved spectra with an optical multichannel analyzer and proton kinetics with pyranine, see ref *19*.

RESULTS

Detection of a New Intermediate between the O and the BR States: Absorption Changes in the Visible. We have investigated the late events in the photocycles of the E194Q and the E204Q mutants, singly, as double mutants, and with several additional mutations. Earlier measurements in the visible (*13*, *14*, *19*) revealed existence of an extremely slow O-like (i.e., red-shifted) intermediate in such mutants, with complete decay only in the time range of several seconds (at ~10 °C and pH 5.0−6.5).

Figure 1A shows absorption changes at 410 nm (for the M state), 570 nm (for depletion of the BR state) and 660 nm (for the O state) after flash photoexcitation of the E9Q/E194Q mutant. The O state (possibly together with N) is

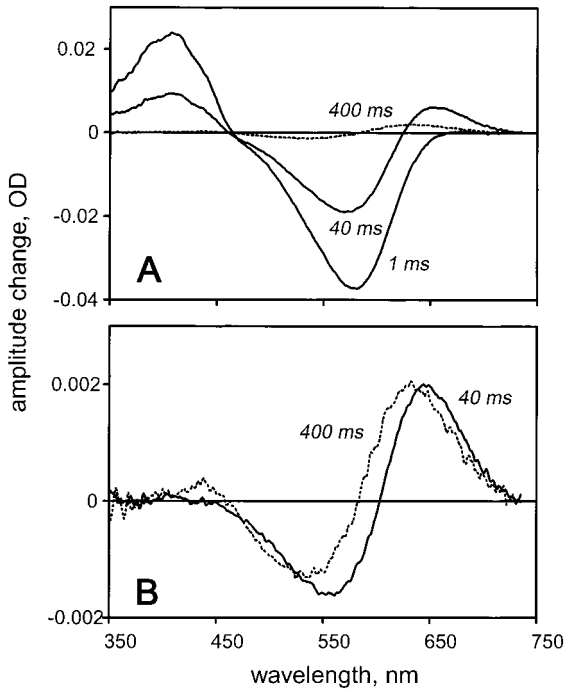

FIGURE 2: Difference absorption spectra at selected times after flash photoexcitation of the E9Q/E194Q mutant. (A) Measured spectra at 1, 40, and 400 ms; conditions as in Figure 1A. (B) Spectrum calculated by interactively subtracting the 1 ms spectrum in panel A from the spectrum at 40 ms until absorption change at 400 nm was minimal (solid line), normalized to and compared with the spectrum at 400 ms in panel A. Similar shifts of the early and late difference spectra were observed with the E194Q/E204Q mutant but with smaller magnitudes (not shown).

formed at the expense of M with a time constant τ_0 of about 15 ms. The major component of the M decay has a time constant τ_1 of several tens of milliseconds. The photocycle is finished with a time constant τ_3 of about 1 s. The absorbance changes contain an additional process, with time constant τ_2 in the hundreds of milliseconds time range, i.e., within the lifetime of the red-shifted (O) intermediate. The transient states that decay with τ_2 and τ_3 have red-shifted absorption maxima and FTIR features indicative of a distorted all-trans chromophore (Figure 2 and below). We designate the new intermediate implied by the additional time constant as O′. Such an additional intermediate was observed (mostly with time-resolved FTIR) in all other mutants tested that contained either the E194Q or the E204Q residue replacements (E194Q, E204Q, E194Q/E204Q, E194D/E204Q, and D96N/E194Q, results not shown). Although the amount of O′ is increased by the additional mutation in E9Q/E194Q, the FTIR spectra of the E9Q single mutant (not shown) indicated that the appearance of the O′ state was not caused by this residue replacement. We used the E9Q/E194Q mutant in all studies described below because (a) the kinetics were favorable for greater accumulation of O′ and (b) the clone containing this gene showed better [4-^{13}C]aspartate labeling.

When Glu-194 or Glu-204 is replaced with a nonprotonatable residue, the proton release to the extracellular surface, which is normally coincident with the rise of the M state, is delayed until the end of the photocycle (*9*, *13*, *14*, *19*). Time-resolved pH measurement with pyranine demonstrate (Figure 1B) that the proton uptake (presumed to occur at the cytoplasmic surface, as in the wild type) is correlated with

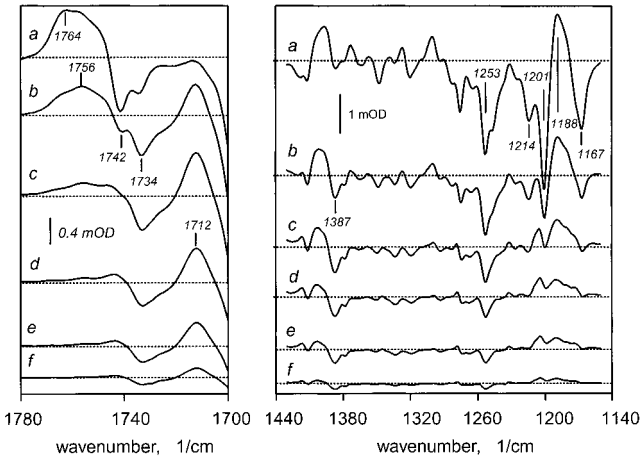

FIGURE 3: Measured FTIR difference spectra at selected times after flash photoexcitation of the E9Q/E194Q mutant. The spectra a−f refer to delay times of 20 ms, 100 ms, 200 ms, 0.5 s, 1 s, and 2 s.

the τ_1 process, while proton release (presumed to occur at the extracellular surface, as in the wild type) is correlated not with τ_2 but with τ_3. The two difference spectra at 40 and 400 ms in the photocycle of E9Q/E194Q, shown in Figure 2, demonstrate that initially the intermediates present are more red-shifted than the states that accumulate later. From the FTIR spectra (see below) it appears that these spectra refer to changing mixtures of O and O′, and the composition of the mixture shifts with τ_2 to predominantly O′. We conclude from the proton kinetics in Figure 1B that the initial mixture of the O and O′ intermediates arises with the proton uptake at the cytoplasmic surface. The results indicate further that proton is not released to the extracellular surface in either O or O′, and therefore, the difference between O and O′ does not reside in the proton release step.

Detection of a New Intermediate between the O and the BR States: Absorption Changes in the Infrared. From time-resolved measurements on E9Q/E194Q at pH 5.3 and 8 °C in both infrared (Figures 3 and 4) and visible regions (as in Figure 1), a combined global analysis yielded the time constants $\tau_1 = 63 \pm 7$ ms, $\tau_2 = 200 \pm 50$ ms, and $\tau_3 = 1.1 \pm 0.2$ s. Extrapolation to zero time (i.e., to before the process with τ_1), produced an FTIR spectrum typical for a mixture of the M, N, and O intermediates (Figure 4, spectrum a). Among the prominent characteristic bands in this early spectrum are (a) a broad maximum for the protonated Asp-85 that consists of bands at 1764 cm^{-1} (from the M state) and at ∼1756 cm^{-1} (from the N and O states), with amplitudes that indicate that approximately half of the molecules in this mixture are still in M; (b) a bilobe (−/+) feature at 1670/1649 cm^{-1} characteristic of the amide I changes in the N state, with low magnitude, presumably because the population of N is small; (c) a strong negative ethylenic band at 1527 cm^{-1} (from the M and N states); (d) negative bands at 1253, 1214, 1201, and 1167 cm^{-1} (indicative of 13-cis configuration of the retinal in the M and N states); (e) a negative carbonyl stretch of Asp-96 at 1742 cm^{-1} (from its deprotonation in the N state); (f) a negative feature at 1734 cm^{-1} due to an environmental change around Asp-115; (g) positive features at 1397 cm^{-1} (symmetric carboxylate stretch of Asp-96) (*28*, *29*) and 1300 cm^{-1} (from the N state); (h) positive features at 1188 cm^{-1} (from the N and O states); and (i) a small positive shoulder of the ethylenic stretch band, at 1506 cm^{-1} (from the O state).

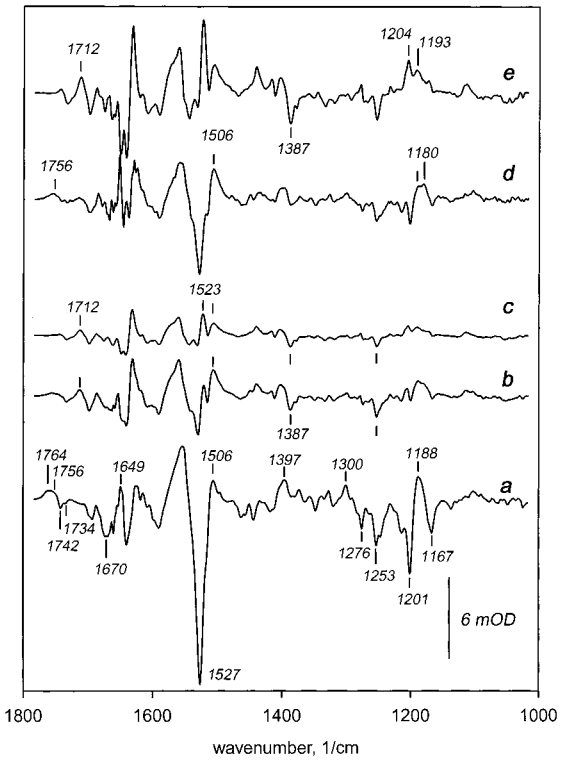

FIGURE 4: Spectra associated with relaxation time constants, from global analysis of measured spectra such as those shown in Figure 3, and calculated spectra for O and O′. The spectra a, b, and c refer to the mixtures of products that decay with time constants τ_1, τ_2, and τ_3. Spectra d and e are the estimated spectra of the O and O′ states, respectively, calculated from spectra b and c as discussed in the text. The spectrum for O, but not O′, may have a contribution from N. Spectra d and e are magnified 2.5× to show details.

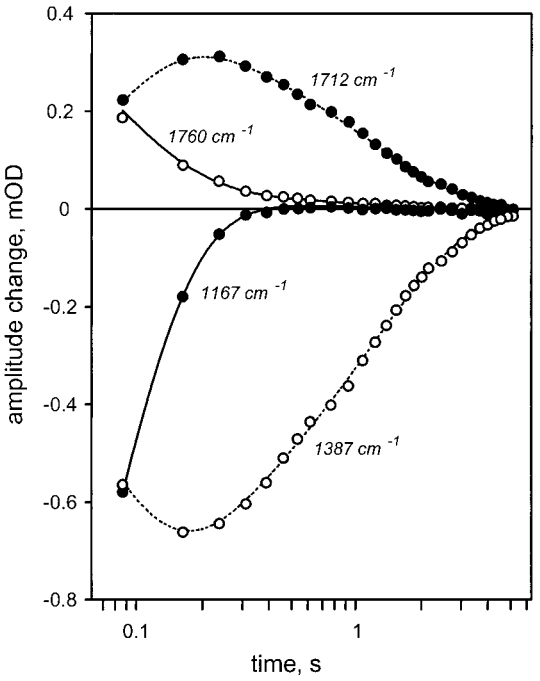

FIGURE 5: Kinetics of IR absorption change at selected frequencies. Data from time-resolved FTIR spectra of E9Q/E194Q mutant were measured as in Figure 3.

The kinetic process that occurs with τ_1 (Figures 3 and 4b) produces changes usually associated (*8*, *22*, *30*) with the accumulation of the O state: (a) shift of the Asp-85 carbonyl stretch to 1756 cm^{-1} (in O, as well as in N) at the expense of decrease of absorption at 1764 cm^{-1} (in M); (b) disappearance of the negative band at 1742 cm^{-1} of Asp-96 because this residue is reprotonated; (c) further increase in the relative amplitude of the band at 1506 cm^{-1}, while the net negative ethylenic stretch loses amplitude and shifts to 1530 cm^{-1}; (d) disappearance of the negative all-trans bands at 1168, 1201, and 1214 cm^{-1} (from reisomerization from 13-cis), accompanied by a decrease in the amplitude of the 1253 cm^{-1} band; and (e) appearance of a positive band at 1180 cm^{-1}. Figure 4, spectrum b has many features of O but it is different, especially in the ethylenic stretch region, where a new shoulder appears at 1523 cm^{-1}. The higher frequency of this putative ethylenic stretch, which increases in relative amplitude with time (Figure 4, spectra b and c) would be consistent with the less red-shifted maximum observed in the visible at 400 ms (Figure 2).

Although the process that occurs with τ_2 (Figure 3, change from spectrum b to spectrum c) represents partial recovery of the BR state, it appears to mark also a redistribution between a more or less authentic O state (or a mixture of N and O) and the O′ intermediate. This is supported by evaluation of the spectra of the individual species. Spectrum d in Figure 4 is the spectrum for O in this system, calculated on the basis that the spectra associated with the decay time constants τ_2 and τ_3 (spectra b and c) are different mixtures of O and O′ and that O, but not O′, contains a C═O stretch band from Asp-85. According to this calculation, spectrum b is a 1:1 mixture of O and O′, but this ratio is 1:4 for spectrum c. The calculated spectrum for O (Figure 4, spectrum d) contains several characteristic features of the spectra reported earlier for the O state (*7*, *22*, *30*). In the published spectra the ethylenic stretch region is dominated by the positive C═C band at 1506 cm^{-1}. Perturbation of the *all-trans*-retinal is indicated by positive bands at about 1168 and 1185 cm^{-1} and a negative band at about 1200 cm^{-1}. In two of the published spectra (*7*, *22*) the band at 1168 cm^{-1} is larger than the one at 1185 cm^{-1}, but in the third (*30*) the amplitude ratio is the reverse. In all spectra for O (*7*, *22*, *30*), the positive band at about 1756 cm^{-1} indicates that Asp-85 is still protonated. Other common features include numerous positive bands on the low-frequency side of the ethylenic stretch region, most prominently the one at about 1395 cm^{-1}. Our calculated spectrum for O agrees with all the consensus features, except that the C−C stretch band is a complex positive feature at 1180/1189 cm^{-1} without a positive band at 1168 cm^{-1}. This, most probably, indicates some contribution from N.

The same calculation yields spectrum e in Figure 4 for O′. In addition to the new positive C = C band at 1523 cm^{-1}, mentioned above, it is distinguished from O by a somewhat changed fingerprint region and more importantly by a strong positive band at 1712 cm^{-1} and a prominent negative band at 1387 cm^{-1} (Figures 3−5). These bands have large relative amplitudes because all other difference bands become smaller by this time in the photocycle. Both bands decay in a biexponential mode with τ_2 and τ_3 (Figure 5). The position of the band at 1712 cm^{-1} makes it a good candidate for a protonated carboxyl group stretch, ν_{COOH}, while the position at 1387 cm^{-1} is consistent with a symmetric carboxylate band, ν_{COO^-}. The protonation process implied by the appearance of these bands occurs concurrently with deprotonation

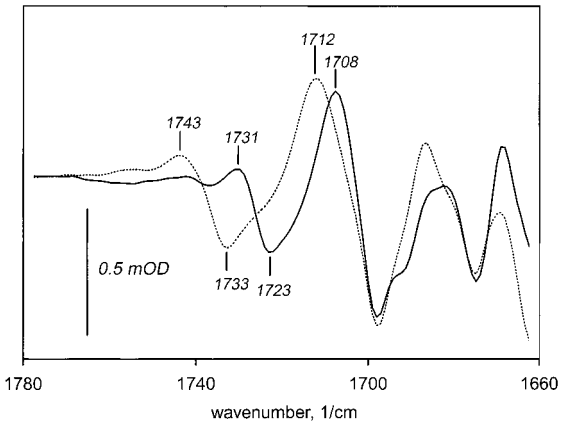

FIGURE 6: Deuterium isotope effect on carboxyl frequency region of the spectrum that decays with the τ_3 time constant. The spectra were calculated as in Figure 4. The dotted line is in H_2O (taken from Figure 4c); the solid line is the same but in D_2O. The latter was obtained by interactive subtraction of the spectrum measured in H_2O from that measured in D_2O-based buffers to compensate for the residual presence of H_2O. Disappearance of the positive band at 1743 cm^{-1} (from the absorption of Asp-115 in H_2O) was taken as the criterion. This method indicated the presence of about 30% H_2O in the D_2O-based buffer.

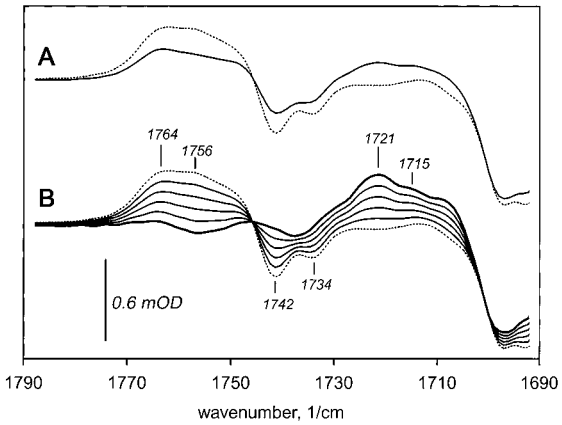

FIGURE 7: Carboxyl stretch frequency region for the spectrum *before* the process with time constant τ_1. (A) Measured spectra for the unlabeled (dotted line) and partly [4-^{13}C]Asp-labeled samples (solid line). (B) Calculated spectrum corresponding to 100% labeling by successive subtractions and renormalization of the unlabeled spectrum from the spectrum of the partly labeled sample. The bold line is the estimated spectrum of the fully labeled [4-^{13}C]-Asp-labeled sample, while the dotted line is the measured spectrum of the unlabeled sample. The lines at intermediate positions illustrate the progress of increasing subtraction. The normalization factor for the spectrum shown in bold was 2.5, corresponding to about 40% labeling, as in ref *25*.

of Asp-85 (decay of the positive bands in the 1756−1760 cm^{-1} region, with τ_1 and τ_2), while the reisomerization of the retinal to all-trans (decay of the negative 1167 cm^{-1} band) is with τ_1 (Figure 5). From this, we conclude, tentatively, that the 1712 and 1387 cm^{-1} bands belong to an acidic residue that acts as the acceptor of the Asp-85 proton. If so, O′ is a state in which Asp-85 and another acidic residue (Asp-212, see Discussion), are deprotonated and protonated, respectively, i.e., reversed relative to authentic O.

Additional mutants tested with slowly decaying O states included E194R, F208N, T205V, and T89A. Bands at 1712 and 1387 cm^{-1}, if present, were not prominent, as also in the wild type (not shown). However, an earlier report (*22*) with very good signal/noise identified an unassigned small-amplitude band at 1712 cm^{-1} both in the wild type at pH 4 and 40 °C (conditions that increase accumulation of the O state) and in E204Q.

Assignment of the Positive 1712 cm^{-1} and the Negative 1387 cm^{-1} Bands to an Aspartic Acid. Earlier, the negative bands at 1742 and at 1734 cm^{-1} from the BR state were assigned to the protonated C═O stretch of Asp-96 and Asp-115, respectively (*20*, *28*, *31*−*33*). We confirmed the assignment of the 1742 cm^{-1} band to Asp-96 in the context of the E194Q mutation, because in the D96N/E194Q mutant this band was absent (not shown). All previously assigned COOH bands (*20*, *28*, *31*, *32*), positive at 1764 and 1756 cm^{-1} (Asp-85), negative at 1742 cm^{-1} (Asp-96) and at 1734 cm^{-1} (Asp-115), exhibited the expected sensitivity to D_2O/H_2O exchange in the spectrum before the τ_1 process. The observed 8 ± 1 cm^{-1} downshift for these bands (not shown) is in accord with both theoretically predicted (see, for instance, ref *34*) and earlier reported deuterium-induced shifts of 9−14 cm^{-1} (*14*, *22*, *25*, *35*−*37*).

For assignment of the 1712 and 1387 cm^{-1} bands the FTIR measurements were performed in D_2O-substituted buffer, as well as with samples labeled with [4-^{13}C]aspartate. The downshift of the 1712 cm^{-1} band in D_2O is only approximately 4 cm^{-1} (Figure 6), i.e., much less than for the other aspartates. However, the well-known 8−10 cm^{-1} shift upon deuteration is typical for carboxylic acids only when not in strong hydrogen bonding [e.g., for Asp-85 in M or in the monomer of propionic acid (*36*)]. For strongly hydrogen-bonded carboxyls such as the cycle dimer of propionic acid (*36*), the measured shift is ∼4 cm^{-1}. Thus, the deuterium-induced shift of the positive 1712 cm^{-1} band is consistent with its origin from a strongly hydrogen-bonded carboxylic acid. Strong hydrogen bonding is expected also from the low frequency of this band. On the other hand, the negative 1387 cm^{-1} band was insensitive to deuterium exchange (not shown), as expected for the symmetric stretch of an unprotonated carboxylate.

The effects of [4-^{13}C]Asp labeling were evaluated both by comparison of the measured spectra for the unlabeled and partially labeled samples and by calculating the estimated spectrum of a fully labeled sample (Figures 7−10). This was done by weighted subtraction of the spectrum of the unlabeled sample (dashed line) from that of a partly labeled one, with the disappearance of bands above about 1730 cm^{-1}, which are assigned to the known aspartic acids, as the criterion. To illustrate the way the spectra with increasing weighting factors approached this limiting condition, we show in Figures 7−10 several calculated spectra in addition to the final one (bold line). In the spectrum before the τ_1 process, [4-^{13}C]Asp labeling produced the following changes: (a) the positive Asp-85 bands (ν_{COOH}) are shifted, as expected, from 1764 (in M) and 1756 cm^{-1} (in N/O) to 1721 and 1715 cm^{-1}, respectively (Figure 7); and (b) a positive band is shifted from 1397 to 1382 cm^{-1} (Figure 8). The position of the 1397 cm^{-1} band and its insensitivity to deuterium exchange (not shown) made it a good candidate for the band of the symmetric COO^- stretch, ν_{COO^-}, of a carboxylic acid. Its sensitivity to [4-^{13}C]Asp labeling and its appearance in our early time-resolved difference spectrum, the one with contribution from N, allowed its unique

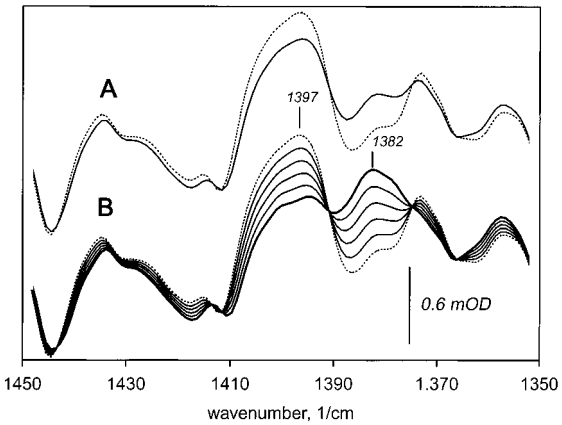

FIGURE 8: Analysis of measured spectra as in Figure 7 but for the region of the symmetric carboxylate stretch region of the vibrations for deprotonated carboxylic acids.

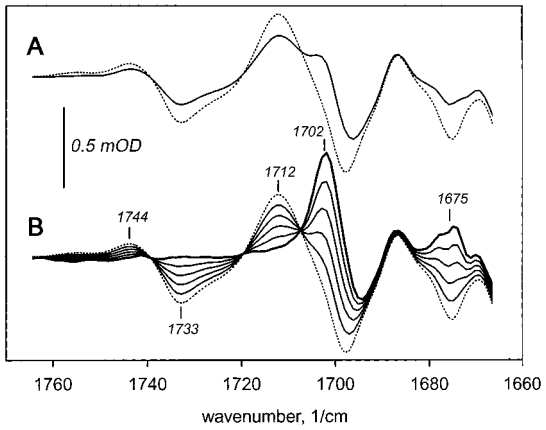

FIGURE 9: Carbonyl stretch frequency region for the spectrum *before* the process with time constant τ_3. (A) Measured spectra for the unlabeled (dotted line) and partly [4-^{13}C]Asp-labeled samples (solid line). (B) Calculated spectrum corresponding to 100% labeling by successive subtractions and renormalization of the unlabeled spectrum from the spectrum of the partly labeled sample. The bold line is the estimated spectrum of the fully labeled [4-^{13}C]-Asp-labeled sample, while the dotted line is the measured spectrum of the unlabeled sample. The lines at intermediate positions illustrate the progress of increasing subtraction. The normalization factor for the spectrum in bold was 2.5, as in Figures 7 and 8. The effective noise in the calculated [4-^{13}C]Asp spectrum is approximately 20× higher below 1680 cm^{-1} than in the unlabeled sample above 1700 cm^{-1}.

assignment to the ν_{COO^-} of Asp-96, consistent with the earlier assignment of a 1399 cm^{-1} band to this mode (*28*, *29*).

In the spectra that contain the O′ intermediate (i.e., before and after the τ_2 process), differences between [4-^{12}C]Asp and [4-^{13}C]Asp samples are evident in both regions that contain bands of carboxyl groups (Figures 9 and 10). Importantly, in the calculated spectrum for the fully labeled sample (bold line), the positive 1712 cm^{-1} band disappears simultaneously with the known aspartate bands at higher frequencies (Figure 9B). This is strong evidence that the 1712 cm^{-1} band also originates from a labeled residue, i.e., an aspartic acid. The ^{13}C-induced shift should move this band to approximately 1670 cm^{-1}. There is indeed a new positive feature at 1675 cm^{-1}, but its assignment as the shifted C═O stretch band in this noisy region is uncertain. The region below approximately 1680 cm^{-1} was difficult to evaluate because of strong difference bands (e.g., the 1670 cm^{-1} band of the perturbed amide I band) and very high noise (due to static absorption from the peptide and water). On the other hand, the conclusion that the positive band at 1712 cm^{-1} is strongly downshifted in the [4-^{13}C]Asp-labeled sample, and belongs therefore to an aspartic acid, is reinforced by the [4-^{13}C]-Asp-induced shift (Figure 10B) of the kinetically coupled negative band in the region of symmetric carboxylate vibrations. This band is clearly downshifted from 1387 to 1371 cm^{-1}.

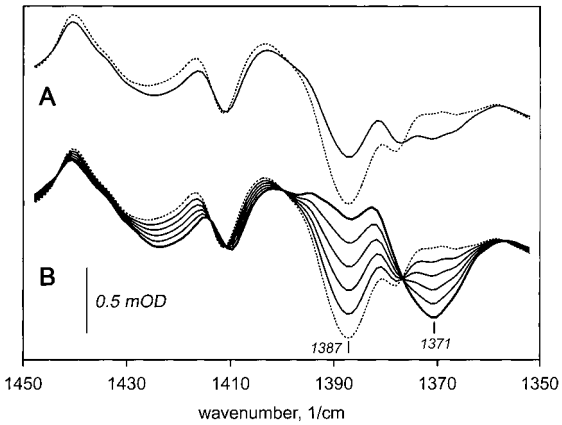

FIGURE 10: Analysis of measured spectra as in Figure 9 but for the region of the symmetric carboxylate stretch region of the vibrations for deprotonated carboxylic acids.

The calculated spectrum for the fully ^{13}C-labeled sample (Figure 9B) reveals, in all samples examined, an additional positive band at 1702 cm^{-1}. Part of this feature comes from the positive band of the Asp-115 (downshifted from 1744 to 1702 cm^{-1} in the [4-^{13}C]Asp sample). The corresponding negative (depletion) feature from Asp-115 is at 1733 cm^{-1} in the unlabeled sample and is shifted to approximately 1694 cm^{-1} upon the ^{13}C labeling. However, the ratio of positive to negative absorption in the [4-^{13}C]Asp-substituted samples is quite different from that in the unlabeled samples, perhaps explained in part by baseline distortion. The magnitude of the feature around 1702 cm^{-1} suggests additional contribution from a previously unobserved band. A possible explanation may be a ^{13}C-induced shift of a negative band, which in the unlabeled sample masks this positive band. A possible candidate for the negative band would be an (unidentified) asparagine. Asparagine carbonyls are known to produce difference bands near 1700 cm^{-1} during the photocycle, e.g., a negative band at 1704 cm^{-1} in the N state (*38*), and should be labeled as much as aspartic acids in the [4-^{13}C]Asp samples (*38*). This possibility would be consistent with the fact that in the partly labeled sample the negative feature at 1697−1691 cm^{-1} is not greater than that of the unlabeled one, although an additional negative contribution from Asp-115 will have shifted to this region. At this time, we cannot uniquely assign the 1702 cm^{-1} band, but this does not affect our assignment of the 1712 and 1387 cm^{-1} bands to Asp-212 (see Discussion).

The magnitudes of the ^{13}C-induced shifts of the ν_{COOH} and ν_{COO^-} bands require comment. The effect of the [4-^{13}C] labeling of aspartic acid on the protonated carboxyl band, ν_{COOH}, can be estimated from very simple considerations (*34*). The expected effect is a downshift of approximately 39 cm^{-1}. This was confirmed experimentally; a shift in ν_{COOH} of 37−41 cm^{-1} was earlier reported for aspartates in bacteriorhodopsin (*14*, *21*, *25*, *33*, *39*). The corresponding estimated

shift for a symmetric carboxylate band, ν_{COO^-}, is 3−4 times smaller. For model compounds, e.g., sodium formate (*25*) or propionic acid (our data, not shown), the ^{13}C label-dependent shift of ν_{COO^-} is 17−27 cm^{-1}. The apparent shifts reported for the ν_{COO^-} bands of aspartates in bacteriorhodopsin are in accord with the above, being on the order of 11−19 cm^{-1} (*33*, *36*, *39*). The shifts we observe for the putative ν_{COO^-} of the aspartates in question, 15 cm^{-1} for Asp-96 and 16 cm^{-1} for Asp-212, are consistent with this.

DISCUSSION

When the proton release pathway to the extracellular surface is blocked by replacement of either Glu-194 or Glu-204 with glutamine, decay of the O to the BR state is greatly slowed, and a intermediate state, termed O′, appears before recovery of the initial BR state. It is less red-shifted than the authentic O state; it contains *all-trans*-retinal like O; but most importantly, unlike in O, Asp-85 is deprotonated and an aspartic acid residue that appears to be Asp-212 is newly protonated.

The evidence for the protonation of an aspartate in O′ is the appearance of a prominent positive band at 1712 cm^{-1} and a coupled negative band at 1387 cm^{-1} (Figures 3−5). Bands near these frequencies are usually attributed to the C═O stretch of a protonated carboxyl and the symmetric stretch of an unprotonated carboxylate, respectively, of an aspartic or glutamic acid. This is consistent with the observed downshift of the 1712 cm^{-1} band (Figure 6), but not the 1387 cm^{-1} band, in D_2O and with the kinetic coupling of the rise and decay of the two bands (Figure 5). Since these bands were present in the D96N/E194Q, E9Q/E194Q, and E204Q mutants, Asp-96, as well as Glu-9, Glu-204, and Glu-194, can be excluded from the list of possible candidates. The same is true for Asp-115, because in the O′ state in the D96N/E194Q mutant (in the presence of 0.1 M NaN_3) the band of the protonated carboxyl of Asp 115 was clearly upshifted from 1732 in BR to 1739 cm^{-1} (not shown) rather than downshifted if it were to contribute to the 1712 cm^{-1} band. Firm assignment of the two bands specifically to an aspartic acid is provided by the isotope shift of both 1712 and 1387 cm^{-1} bands in [4-^{13}C]Asp-labeled samples (Figures 9 and 10).

The only residues that remain as candidates for these bands are Asp-36, Asp-38, Asp-102, Asp-104, Asp-85, and Asp212. The first four are at the cytoplasmic surface and are unlikely to be the source of the bands. According to the structure of the protein (*6*, *40*−*43*), all four aspartic acids are fully exposed to the medium and at the high salt concentration used should have largely unperturbed pK_as, i.e., at or below 5. The amplitude of the 1712 cm^{-1} band was found to be practically invariant at pH values of 5.3, 6.3, and 7.0 in E194Q/E204Q (data not shown). Because the carboxyl group in question is nearly unaffected by bulk pH in this range, it could hardly be attributed to a surface-exposed residue. We have recently shown that replacement of any of the four surface aspartic acids with asparagine has very little effect on the photocycle (*44*).

Importantly, the formation of the positive 1712 cm^{-1} band is kinetically coupled to the disappearance of the protonated bands of Asp-85 at 1764 and 1756 cm^{-1} (Figures 3 and 5).

Table 1: Protonated Carboxyl (ν_{COOH}) and Carboxylate (ν_{COO^-}) Stretch Frequencies of Functional Aspartic Acid Residues in Intermediates of the Photocycles of Bacteriorhodopsin Mutants E194Q and E204Q[a]

state/ residue	stretch frequency (cm^{-1})			
	Asp-85	Asp-96	Asp-115	Asp-212
bR	no signal	1742 (Δ ∼ 44)	1733 (Δ = 39)	1387 (Δ = 16)*
M	1764 (Δ = 43)	no info	1748[b] (Δ = 40)	no signal
N	1756 (Δ = 41)	1397 (Δ = 15)*	1748[b] (Δ = 40)	no signal
O	1756 (Δ = 41)	∼1738	1748 (Δ ∼ 40)	no signal
O′	no signal	no info	1744 (Δ ∼ 42)	1712 (Δ ∼ 37)

[a] The [4-^{13}C]Asp-induced shifts are given in parentheses. Symmetric carboxylate, ν_{COO^-}, stretch frequencies are marked with an asterisk. "No signal" refers to the absence of detectable signal when a particular residue is in the same protonation/environmental state as in the BR state (Asp-212 in M, Asp-96 in O, Asp-85 in O′). "No info" refers to insufficient data for assignment in this study. [b] This frequency is a mean of two frequencies obtained by decomposition of the protonated carbonyl region in Figure 7 into Gaussian components, which resulted in two bands at 1746 and at 1751 cm^{-1}. We do not have sufficient information to attribute any of these specifically to either M or N.

There would be two alternative means for such coupling: (a) protonation of another aspartic acid by Asp-85 or (b) shift of the existing ν_{COOH} bands of the protonated Asp-85 to 1712 cm^{-1} as a result of stronger hydrogen bonding, which would (*45*, *46*) cause a strong downshift of ν_{COOH}. The two remaining candidates for origin of the newly detected bands, which correspond to these alternatives, are therefore Asp-212 (protonation) and Asp-85 (change of hydrogen bonding). Assignment of the bands in the usual way, i.e., from their presence or absence in Asp-85 and Asp-212 mutants, is not possible because these mutants are highly perturbed (e.g., refs *24* and *47*). However, the results with [4-^{13}C]Asp-labeled samples (Figures 9 and 10) do decide between the two alternatives. If the 1712 cm^{-1} band is the carbonyl stretch, ν_{COOH}, of the protonated Asp-85 in O′, which is downshifted from 1756 cm^{-1} in O by increased hydrogen-bonding in the O → O′ transition, its kinetic coupling to the band at 1387 cm^{-1} is apparent and coincidental. In this case, the 1712 and 1387 cm^{-1} bands originate from different residues and entirely different modes, and therefore the former but not the latter should be affected by [4-^{13}C] labeling of aspartic acids. On the other hand, if the 1712 cm^{-1} band originates from Asp-212, both bands should be sensitive to ^{13}C labeling, and the 1387 cm^{-1} band is then identified as a symmetric carboxylate stretch that indicates disappearance of an unprotonated carboxylate group. This is indeed as found (Figure 10).

Table 1 summarizes the band assignments for protonated, ν_{COOH}, and deprotonated (symmetric), ν_{COO^-}, stretch frequencies of all functional aspartic acid residues during the later part of the photocycle in the E194Q and E204Q family of mutants and their sensitivities to [4-^{13}C]Asp substitution. Our data on ν_{COOH} Asp-85, Asp-96, and Asp-115 in these mutants are in accord with the previously published results for the wild type and for other mutants. The previously reported [4-^{13}C]Asp-induced shifts of the ν_{COOH} of Asp-85 (*21*, *25*) and Asp-96 (*25*, *39*) (the 1740 cm^{-1} band was not yet assigned to Asp-96 at that time) are also in accord with our data. Although predicted, the ^{13}C labeling-dependent shift of Asp-115 bands has not been reported before. The assignment of the two Asp-212 bands, as well as their sensitivity to [4-^{13}C]Asp substitution, are entirely new.

Various frequencies have been proposed before for the protonated C=O stretch band of Asp-212. At first, a band at 1738 cm^{-1} was assigned to the ν_{COOH} of Asp-212 (*31*, *48*, *49*), but this was later challenged (*20*, *21*). A recent assignment of 1731 cm^{-1} as the frequency of ν_{COOH} of Asp-212 was from spectroscopic titration to very low pH (*50*), from the consideration that this residue should have the lowest pK_a of all acidic residues. At such a pH Asp-85 is protonated, a condition that would affect the hydrogen-bonding state of Asp-212 and therefore the frequency of its C=O stretch band. Interestingly, the appearance of another band at 1713 cm^{-1} at low pH was also observed but not further discussed (*50*). For the symmetric COO^- stretch the frequency of 1393 cm^{-1} in M and N was proposed by Fahmy et al. (*21*). The latter was reported to shift to 1374 cm^{-1} upon [4-^{13}C]Asp substitution.

Three different kinetic models could account for the observed time-resolved spectroscopic changes: (a) a sequential scheme with back-reactions (M ↔ N ↔ O ↔ O′ → BR), (b) a branched scheme with the possibility of back-reactions (M ↔ N ↔ O → BR, and M ↔ N ↔ O′ → BR), and (c) a scheme with O′ in a *cul-de-sac* (M ↔ N ↔ O → BR and O ↔ O′). Mathematically, these are indistinguishable because they all produce apparent four-exponential kinetics (three-exponential in the time range of the FTIR measurements). Since the absolute spectra are not known and the number of possible intrinsic rate constants exceeds that of the measured apparent ones, it is impossible to firmly reject any of these schemes. On the other hand, the three schemes have different implications for the photocycle mechanism. The first, sequential scheme implies that, in the family of Glu-194/Glu-204 mutants at least, the proton of Asp-85 passes through Asp-212 on its way to the extracellular surface, and in O′ we are trapping a state after protonation of Asp-212, but before its, now slower, deprotonation. The other two schemes imply that the observed proton equilibration between Asp-85 and Asp-212 is not an obligatory step in the conduction of the proton to the surface. Another question is whether such proton equilibration is an exclusive property of the mutants we have studied. The fact that a small (then unassigned) band at 1712 cm^{-1} was noted earlier in the O intermediate (or in a mixture of O and O′) during the wild-type photocycle (*22*) suggests that transient protonation of Asp-212 might have physiological significance for the wild type as well. The fact that the band was detected in the wild type at pH 4 (*22*) but not at higher pH (*30*) suggests further that protonation of Asp-212 might have to do with lack of early proton release in the photocycle, as in the mutants we describe here.

REFERENCES

1. Lanyi, J. K. (1993) *Biochim. Biophys. Acta Bio-Energ. 1183*, 241−261.
2. Lanyi, J. K. (1997) *J. Biol. Chem. 272*, 31209−31212.
3. Oesterhelt, D. (1998) *Curr. Opin. Struct. Biol. 8*, 489−500.
4. Balashov, S. P., Imasheva, E. S., Govindjee, R., and Ebrey, T. G. (1996) *Biophys. J. 70*, 473−481.
5. Rammelsberg, R., Huhn, G., Lübben, M., and Gerwert, K. (1998) *Biochemistry 37*, 5001−5009.
6. Luecke, H., Richter, H. T., and Lanyi, J. K. (1998) *Science 280*, 1934−1937.
7. Kandori, H., Yamazaki, Y., Hatanaka, M., Needleman, R., Brown, L. S., Richter, H. T., Lanyi, J. K., and Maeda, A. (1997) *Biochemistry 36*, 5134−5141.
8. Richter, H. T., Needleman, R., Kandori, H., Maeda, A., and Lanyi, J. K. (1996) *Biochemistry 35*, 15461−15466.
9. Richter, H. T., Brown, L. S., Needleman, R., and Lanyi, J. K. (1996) *Biochemistry 35*, 4054−4062.
10. Balashov, S. P., Govindjee, R., Kono, M., Imasheva, E., Lukashev, E., Ebrey, T. G., Crouch, R. K., Menick, D. R., and Feng, Y. (1993) *Biochemistry 32*, 10331−10343.
11. Cao, Y., Brown, L. S., Sasaki, J., Maeda, A., Needleman, R., and Lanyi, J. K. (1995) *Biophys. J. 68*, 1518−1530.
12. Govindjee, R., Misra, S., Balashov, S. P., Ebrey, T. G., Crouch, R. K., and Menick, D. R. (1996) *Biophys. J. 71*, 1011−1023.
13. Balashov, S. P., Imasheva, E. S., Ebrey, T. G., Chen, N., Menick, D. R., and Crouch, R. K. (1997) *Biochemistry 36*, 8671−8676.
14. Dioumaev, A. K., Richter, H. T., Brown, L. S., Tanio, M., Tuzi, S., Saitô, H., Kimura, Y., Needleman, R., and Lanyi, J. K. (1998) *Biochemistry 37*, 2496−2506.
15. Maeda, A., Kandori, H., Yamazaki, Y., Nishimura, S., Hatanaka, M., Chon, Y. S., Sasaki, J., Needleman, R., and Lanyi, J. K. (1997) *J. Biochem. (Tokyo) 121*, 399−406.
16. Balashov, S. P., Lu, M., Imasheva, E. S., Govindjee, R., Ebrey, T. G., Othersen, B. I., Chen, Y., Crouch, R. K., and Menick, D. R. (1999) *Biochemistry 38*, 2026−2039.
17. Liu, S. Y. (1990) *Biophys. J. 57*, 943−950.
18. Le Coutre, J., and Gerwert, K. (1996) *FEBS Lett. 398*, 333−336.
19. Brown, L. S., Sasaki, J., Kandori, H., Maeda, A., Needleman, R., and Lanyi, J. K. (1995) *J. Biol. Chem. 270*, 27122−27126.
20. Sasaki, J., Lanyi, J. K., Needleman, R., Yoshizawa, T., and Maeda, A. (1994) *Biochemistry 33*, 3178−3184.
21. Fahmy, K., Weidlich, O., Engelhard, M., Sigrist, H., and Siebert, F. (1993) *Biochemistry 32*, 5862−5869.
22. Zscherp, C., and Heberle, J. (1997) *J. Phys. Chem. B 101*, 10542−10547.
23. Oesterhelt, D., and Stoeckenius, W. (1974) *Methods. Enzymol. 31*, 667−678.
24. Needleman, R., Chang, M., Ni, B., Váró, G., Fornes, J., White, S. H., and Lanyi, J. K. (1991) *J. Biol. Chem. 266*, 11478−11484.
25. Engelhard, M., Gerwert, K., Hess, B., Kreutz, W., and Siebert, F. (1985) *Biochemistry. 24*, 400−407.
26. Dioumaev, A. K. (1997) *Biophys. Chem. 76*, 1−26.
27. Chizhov, I., Chernavskii, D. S., Engelhard, M., Mueller, K. H., Zubov, B. V., and Hess, B. (1996) *Biophys. J. 71*, 2329−2345.
28. Bousché, O., Braiman, M. S., He, Y.-W., Marti, T., Khorana, H. G., and Rothschild, K. J. (1991) *J. Biol. Chem. 266*, 11063−11067.
29. Pfefferlé, J.-M., Maeda, A., Sasaki, J., and Yoshizawa, T. (1991) *Biochemistry 30*, 6548−6556.
30. Hessling, B., Souvignier, G., and Gerwert, K. (1993) *Biophys. J. 65*, 1929−1941.
31. Braiman, M. S., Mogi, T., Marti, T., Stern, L. J., Khorana, H. G., and Rothschild, K. J. (1988) *Biochemistry 27*, 8516−8520.
32. Gerwert, K., Hess, B., Soppa, J., and Oesterhelt, D. (1989) *Proc. Natl. Acad. Sci. U.S.A. 86*, 4943−4947.
33. Fahmy, K., Weidlich, O., Engelhard, M., Tittor, J., Oesterhelt, D., and Siebert, F. (1992) *Photochem. Photobiol. 56*, 1073−1083.
34. Craver, C. D. (1986) *The Coblentz Society Desk Book of Infrared Spectra*, 2nd ed., Coblentz Society, Kirkwood, MO.
35. Gerwert, K., Ganter, U. M., Siebert, F., and Hess, B. (1987) *FEBS Lett. 213*, 39−44.
36. Maeda, A., Sasaki, J., Shichida, Y., Yoshizawa, T., Chang, M., Ni, B., Needleman, R., and Lanyi, J. K. (1992) *Biochemistry 31*, 4684−4690.
37. Kluge, T., Olejnik, J., Smilowitz, L., and Rothschild, K. J. (1998) *Biochemistry 37*, 10279−10285.
38. Sasaki, J., Shichida, Y., Lanyi, J. K., and Maeda, A. (1992) *J. Biol. Chem. 267*, 20782−20786.
39. Eisenstein, L., Lin, S.-L., Dollinger, G., Odashima, K., Termini, J., Konno, K., Ding, W.-D., and Nakanishi, K. (1987) *J. Am. Chem. Soc. 109*, 6860−6862.

40. Grigorieff, N., Ceska, T. A., Downing, K. H., Baldwin, J. M., and Henderson, R. (1996) *J. Mol. Biol. 259*, 393−421.
41. Kimura, Y., Vassylyev, D. G., Miyazawa, A., Kidera, A., Matsushima, M., Mitsuoka, K., Murata, K., Hirai, T., and Fujiyoshi, Y. (1997) *Nature 389*, 206−211.
42. Pebay-Peyroula, E., Rummel, G., Rosenbusch, J. P., and Landau, E. M. (1997) *Science 277*, 1676−1681.
43. Essen, L. O., Siegert, R., Lehmann, W. D., and Oesterhelt, D. (1998) *Proc. Natl. Acad. Sci. U.S.A. 95*, 11673−11678.
44. Brown, L. S., Needleman, R., and Lanyi, J. K. (1999) *Biochemistry 38*, 6855−6861.
45. Bellamy, L. J. (1975) *Advances in infrared group frequencies*, Chapman and Hall, London.
46. Dioumaev, A. K., and Braiman, M. S. (1995) *J. Am. Chem. Soc. 117*, 10572−10574.
47. Kataoka, M., Kamikubo, H., Tokunaga, F., Brown, L. S., Yamazaki, Y., Maeda, A., Sheves, M., Needleman, R., and Lanyi, J. K. (1994) *J. Mol. Biol. 243*, 621−638.
48. Rothschild, K. J., Braiman, M. S., He, Y.-W., Marti, T., and Khorana, H. G. (1990) *J. Biol. Chem. 265*, 16985−16991.
49. Bousché, O., Sonar, S., Krebs, M. P., Khorana, H. G., and Rothschild, K. J. (1992) *Photochem. Photobiol. 56*, 1085−1095.
50. Kelemen, L., Galajda, P., Száraz, S., and Ormos, P. (1999) *Biophys. J. 76*, 1951−1958.

BI990873+